Korean J. Chem. Eng., **28**(12), 2344-2350 (2011)
DOI: 10.1007/s11814-011-0097-2

Preparation and characterization of activated carbons for SO_2 adsorption from Taixi anthracite by physical activation with steam

Yuwen Zhu, Jihui Gao†, Yang Li, Fei Sun, and Yukun Qin

School of Energy Science and Engineering, Harbin Institute of Technology, Harbin 150001, P. R. China
(*Received 11 December 2010 • accepted 11 April 2011*)

Abstract–Taixi anthracite was used as a precursor to prepare activated carbons (AC) for SO_2 adsorption from flue gas. In this work the activated carbons were prepared by physical activation with steam. Specifically, the effects of activation temperature and burn-off degree on the physico-chemical properties of the resulting AC samples were comparatively studied. The different types of pore volumes, pore size distributions and surface chemistries of the activated carbons on the SO_2 adsorption were also analyzed. The results show that the increasing burn-off leads to samples with continuous evolution of all types of pores except ultramicropore. The ultramicropore volume increases to a maximum of 0.169 cm^3/g at around 50% burn-off and then decreases for 850 °C activation. At higher activation temperature, the micropore volume decreases and the mesopore structure develops to a certain extent. For all the resulting AC samples, the quantities of the basic surface sites always appear much higher than the amount of the acidic sites. The activated carbon prepared with higher micropore volume, smaller median pore diameter and higher quantities of the basic surface sites represents better SO_2 sorption property.

Key words: Activated Carbon, Steam Activation, Textural Properties, Surface Properties, SO_2 Adsorption

INTRODUCTION

Flue gases from combustion of fossil fuels and incineration of solid waste contain significant quantities of sulfur dioxide (SO_2) and nitrogen oxides (NO_x), which constitute a primary source of acid rain [1-3]. In a practical process, the techniques for SO_2 removal are mainly based on the principle of absorption or chemical reactions [4]. Carbon-based flue gas desulfurization technologies based on adsorption of SO_2 and catalytic conversion of SO_2 to sulfuric acid have been explored and applied [5,6]. Activated carbons have been shown to be effective adsorbents for SO_2 in the presence of oxygen and moisture. It is important to know the influence of physico-chemical characteristics of the carbon material on the adsorption and subsequent oxidation of the SO_2 [7,8]. Development of suitable porosity and effectual surface chemistry depends on the precursors as well as the preparation methods.

Chemical activation is normally used in cellulosic materials and to a lesser extent of coals, involving reaction with a chemical reagent such as $ZnCl_2$, KOH, NaOH and phosphoric acid [9]. The usual choices of physical activation gas are steam, CO_2, air, or their mixtures. Due to the endothermic nature of the reactions between char and steam or CO_2, the rate of carbon burn-off can be controlled more easily in comparison to the reactions between char and air which are exothermic. Therefore, steam and CO_2 are preferred for activation in production of activated carbons [10,11].

In a wide range of coal precursors, anthracites are of concern for their abundance, high carbon content and already existing micropores [12]. Microporous activated carbons from anthracites have already been prepared by different methods either with physical activation or with chemical activation in previous studies. However, as the diversity of anthracites, the characteristics of the resulting activated carbons are different, and they are also controlled by various preparation conditions.

In recent years, to promote the adsorption capacity and adsorption kinetics for SO_2 there are many researches on treatment of precursors and the resulting activated carbons to obtain optimal pore structure and surface chemistry. It is effective to improve the SO_2 capabilities of the activated carbons, but the production costs become higher and that leads to a limited application. The overall objective of this work is to prepare steam-activated carbons from Taixi anthracite with optimal SO_2 removal characteristics at low production costs. The initial focus is to explore the differences in texture and surface chemistry of the activated carbons (AC) prepared under a wide range of activation conditions. An attempt is also made to relate certain physico-chemical characteristics to the SO_2 adsorption capacity of the AC sample.

EXPERIMENTAL SECTION

1. Preparation of Activated Carbon

The Taixi anthracite used in this study was obtained from the Ningxia Hui Autonomous Region, China. It is suitable for preparing activated carbon due to its abundance, high carbon content and low ash content. The proximate and ultimate analyses of the anthracite are shown in Table 1. All the raw anthracite received was dried for 12 h in an oven at 110 °C, sieved to a size range of 0.25-0.38 mm, and stored in a desiccator.

†To whom correspondence should be addressed.
E-mail: gaojh@hit.edu.cn
‡This work was presented at the 8th Korea-China Workshop on Clean Energy Technology held at Daejeon, Korea, Nov. 24-27, 2010.

Table 1. Proximate and ultimate analyses of tested sample

Proximate analysis (wt%) (ad)		Ultimate analysis (wt%) (ad)	
Moisture	0.21	C	88.76
Volatile	8.86	H	3.38
Ash	3.4	O	3.17
Fixed carbon	87.53	N	0.85
		S	0.23

The activated carbons were prepared following two stages: carbonization of raw anthracite and subsequent steam activation. Basically, 30 g of anthracite was placed in a quartz tubular reactor (23 mm diameter and 400 mm effective length) placed in a horizontal electrically heated furnace. Temperature control for the tubular reactor consisted of a three-zone temperature control system, and it contained three independent digital temperature controllers. Carbonization was carried out by heating to 700 °C at a rate of 8 °C/min under a constant N_2 flow of 400 ml/min and maintaining for 40 min. Then, the reactor was heated at a constant heating rate of 8 °C/min to the desired activation temperature (800, 850, 900 and 950 °C), and in a steam constant flow for the appropriate time, in order to obtain burn-offs within the range 10-75 wt%. The activated carbons were then cooled to room temperature under nitrogen atmosphere. For steam activation, the flow of water was controlled to generate 0.32 ml/min with a peristaltic pump, evaporated by heater swept with 80 ml/min of N_2. N_2 used was stored in a high-pressure stainless steel cylinder, and was of high purity (99.999%).

On completion, all the resultant activated carbons were weighed to determine their burn-offs and stored in a desiccator. The values reported were an average of two or three accurate experimental measurements. The burn-off, related to the activation step, is the ratio between the weight of fixed carbon reacted and the initial char weight. The yield is the ratio between the final weight of activated carbon and the initial coal weight [7]. The activated carbons produced through steam activation are named as series S. The notations used for the activated carbons are S(activation temperature)-(burn-off).

2. Characterization of the Samples

An accelerated surface area and porosity analyzer (ASAP 2020, Micromeritics) was used for measurement of micropore and mesopore surface areas and pore volumes. N_2 was used at analysis temperature of 77 K, and the adsorption data were obtained over the relative pressure, p/p_0, range from 10^{-7} to 1. Before any such analysis, the sample was degassed under vacuum at 473 K for 10 h. The Brunauer-Emmett-Teller (BET) surface areas (S_{BET}) of the AC samples were calculated from the N_2 adsorption isotherms using the BET equation and are given in Table 2 [13]. The micropore area (S_{mic}) was calculated using *t*-plot method [14]. The micropore volume (V_{mic}) (size<2 nm), median pore diameter (D_{med}) and differential pore volume were estimated by the Horvath-Kawazoe (HK) method [15]. The mesopore volumes (V_{mes}) (size 2-50 nm) and pore size distributions of the AC samples have been calculated by applying Barrett-Joyner and Halenda (BJH) method. The total pore volume (V_{tot}) was calculated from the amount adsorbed at 0.975 relative pressure, and the results are given in Table 2.

The surface functional groups on the activated carbons were analyzed by a Fourier transform infrared (FTIR) spectroscope. A Nicolet Magna-IR 560 E.S.P spectrometer in the range 4,000-400 cm^{-1} with a resolution of 4 cm^{-1}, using pressed KBr pellets which contained approximately 0.5 wt% carbons, was used to realize the measurements. The quantities of surface groups with acidic and basic characteristics were detected comparatively based on the selective neutralization by equilibrium with an alkali and an acid. The number of the acidic sites was determined by Boehm titration under the assumptions that NaOH neutralizes carboxylic, lactonic and phenolic groups (with 0.01 mol/L NaOH solution). The number of surface groups with basic characteristics was detected though the sorption of alcoholic solution of benzoic acid (0.01 mol/L).

3. SO_2 Adsorption Capacity

The SO_2 adsorption experiments were performed in a fixed bed reactor using 2.5 g of sample at 80 °C. The experimental system consists of a tubular reactor (20 mm diameter), placed in a vertical furnace, with a system of valves and mass flow controllers in order to select the flow and the composition of the inlet gas. The gas volumetric composition used in experiments was as follows: SO_2, 1,500 ppm; O_2, 5%; water vapor, 10%; N_2, balance. The SO_2 concentration was continuously monitored with an on-line Fourier transform infrared (FTIR) gas analyzer (GASMET-DX4000, Finland) until 90% penetration. The amount of SO_2 removed expressed in mg SO_2 g^{-1} carbon was calculated by integration of SO_2 conversion versus

Table 2. Physical characteristics of some typical resulting activated carbons

Sample	Activation time (h)	Yield (%)	S_{BET} (m^2/g)	S_{mic} (m^2/g)	V_{tot} (cm^3/g)	V_{mic} (cm^3/g)	D_{med} (Å)
S800-30.2	3.1	64.3	598	513	0.320	0.298	6.67
S850-13.6	0.75	80.2	274	252	0.125	0.124	6.17
S850-23.7	1.3	70.9	453	367	0.223	0.203	6.54
S850-30.9	2	64.2	537	435	0.258	0.239	6.73
S850-40.5	2.7	55.3	730	497	0.353	0.311	7.20
S850-49.5	3.7	46.4	919	597	0.447	0.389	7.42
S850-62.1	4.9	35.2	1153	583	0.562	0.457	7.87
S850-74.3	5.8	23.6	1333	260	0.698	0.490	8.25
S900-31.8	1.3	63.4	408	280	0.200	0.176	6.86
S900-60.4	2.8	37.7	984	429	0.488	0.389	7.91
S950-29.2	1	66.7	366	213	0.183	0.154	7.17
S950-63.8	2.2	33.5	793	223	0.417	0.298	7.94

time curves.

RESULTS AND DISCUSSION

1. Analysis of Textural Characterization

Evaluation of porosity is very important in understanding the adsorptive property of an activated carbon [16,17]. Specifically, micropore volume and surface area could indicate the adsorption capacity of gaseous adsorbates (vapor and SO_2); mesopore volume gives an indication of transits of the reacting gaseous molecules into the internal carbonaceous matrices and the space to store sulfuric acid produced by the reaction.

Fig. 1 shows some of the N_2 adsorption-desorption isotherms for the activated carbons resulting from the steam activation of chars at different activation temperatures (850, 900 and 950 °C). All these isotherms are clearly of Type I, according to IUPAC classification, that are typical of microporous materials. The activated carbons present an increase in amount of N_2 adsorbed with an increase of burn-off (within the range 13-75%). From Fig. 1(a), for low burn-offs the knees of the isotherms are sharp and the plateaus are fairly horizontal that the activated carbons are mainly microporous. As Fig. 1(b) shows, for high burn-offs the amount of N_2 adsorbed increases and the knee becomes broader, which indicates the presence of wider micropores [18].

The isotherms always contain two parts in the range of relative pressure, p/p_0, from 0.2 to 1.0, i.e., adsorption isotherm and desorption isotherm. From Fig. 1(a), there seem to be scarcely any hysteresis loops shown. However, with an increase of burn-off, the plateau of the isotherm becomes steeper, and the hysteresis loop is more obvious, which indicates existing mesoporosity. To see this trend more clearly, we magnify the hysteresis loop of S850-74.3 in Fig. 1(d).

Fig. 1(c) shows the N_2 adsorption isotherms for the activated carbons produced at different activation temperatures with similar burn-off (around 62%). The porous structures produced in steam are very influenced by activation temperature. The activated carbons obtained at lower temperature present an increase in amount of N_2 adsorbed in comparison to that of ACs prepared at higher temperature. It indicates the higher activation temperature developed lower porous structure.

The N_2 BET surface areas (S_{BET}) of the AC samples, included in Table 2, increase with increasing burn-off degree for 850 °C activation. In contrast, the micropore area (S_{mic}) reaches a maximum of 597 m^2/g at 49.5% burn-off and then obviously decreases to 260 m^2/g at 74.3% burn-off. This decrease could be associated with widening micropores. On the other hand, the increase of activation temperature results in a decrease in the S_{BET} and S_{mic} for resulting activated carbons.

To complete the analysis of the porosity development of the AC samples, the results of different pore volumes have been plotted in Fig. 2. As Fig. 2(a) shows, activation with steam at 850 °C pro-

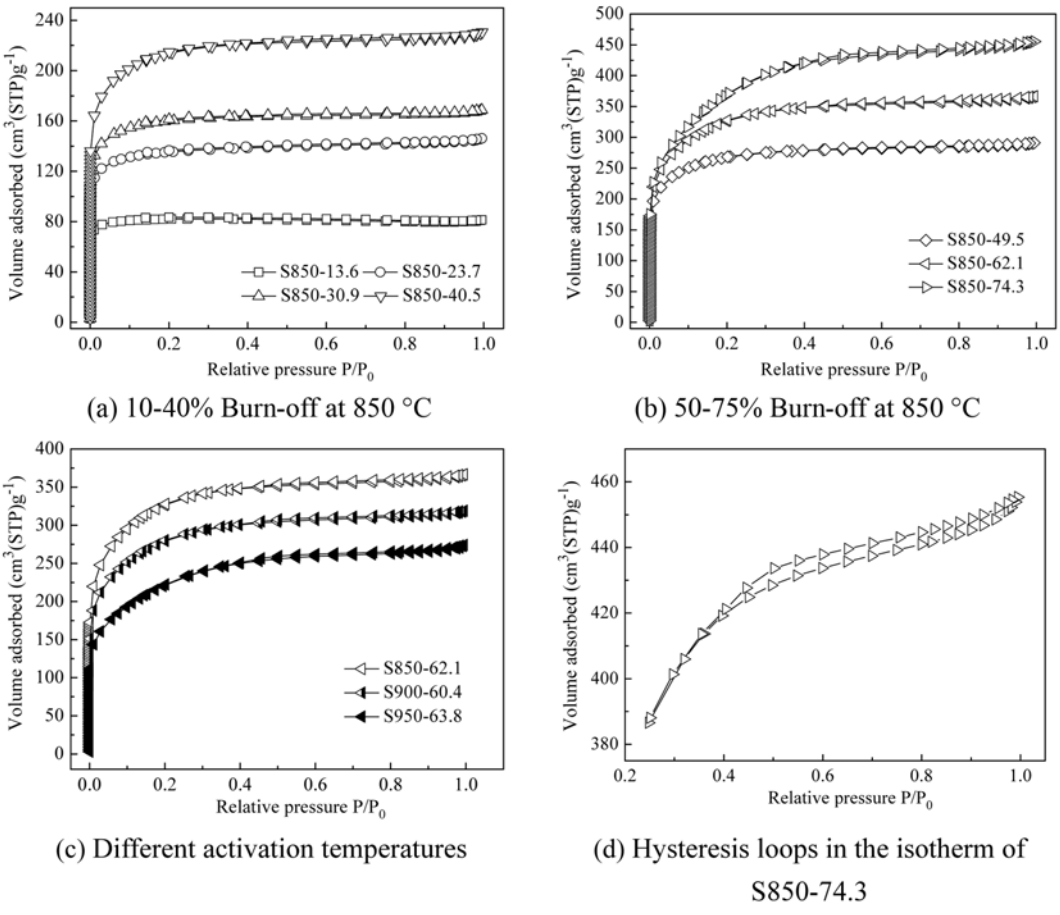

Fig. 1. N_2 adsorption-desorption isotherms for activated carbons.

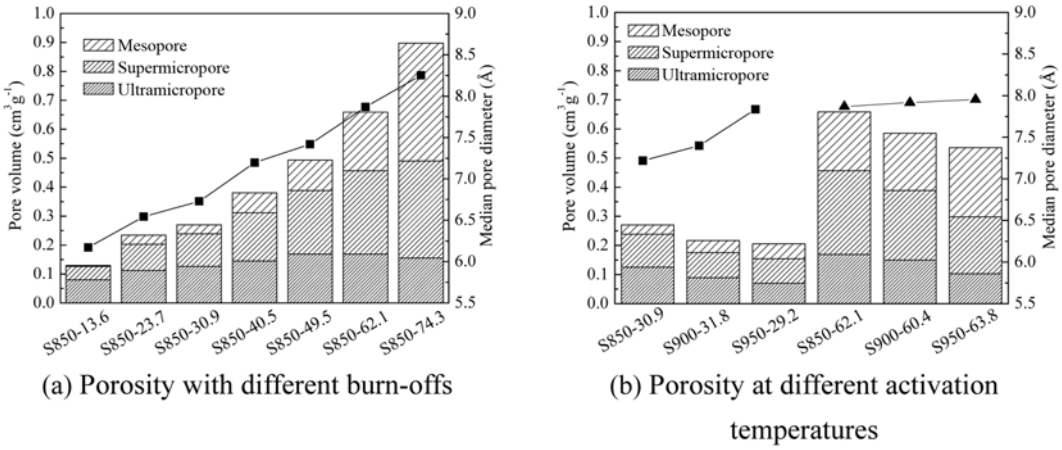

Fig. 2. Histogram of the different types of pores for AC samples.

duces a development of the total porosity. However, the ultramicropore (size<0.7 nm) volume increases to 0.169 cm^3/g from the char up to 49.5% burn-off, then the development is stopped and its volume decreases from 0.169 to 0.155 cm^3/g with an increase in the burn-off from 62.1% to 74.3%. Compared with development of ultramicropore, there is a continuous increase in the volume of supermicropore (size 0.7-2 nm). This means that widening of existing ultramicropores occurs during the whole stage of activation. On the other hand, the mesopore volume increases from the initial stages of activation, and its development is more important from about 40% burn-off. For high burn-off it increases significantly from 0.070 to 0.407 cm^3/g with an increase in the burn-off from 40.5% to 74.3%. This increase can be associated with enlargement of micropores into mesopores progressively, instead of creating a large number of new micropores in the initial activation process.

In particular, the evolution of micropore volumes results in an increase in the median pore diameter. The median pore diameter (D_{med}) gives an indication of the average size of the micropores. The D_{med} calculated by the HK method increases from 6.17 to 8.25 Å due to increase in the burn-off from 13.6% to 74.3%.

As shown in Fig. 2(b), the porosity of activated carbons decreases by increasing activation temperature. In particular, the total micropore volumes strongly reduce from the activation temperature up to 950 °C, while the mesopore volumes increase in a certain extent. Some authors have pointed out that "if the activation removes carbon atoms from the interior of the particle, the result will be the opening up of closed micropores and the enlargement of opened micropores, while burn-off outside of the particle will not result in the development of new porosity, but only in the reduction of particle size" [19]. In this work, the higher activation temperature makes faster gasification rate and lower micropore volume. In other words, at higher temperatures (900 and 950 °C), the reaction is prone to external burn-off and only the most accessible pore structure. Simultaneously, the increase of activation temperature results in an increase in the median pore diameter.

2. Analysis of Surface Chemical Characterization

Surface chemistry of activated carbon plays an important role in adsorption of gases including SO_2 [20-22]. Fig. 3 shows the quantities of surface sites with acidic or basic characteristics (detected by adsorption of NaOH solution or benzoic acid) versus the burn-off and activation temperature. As Fig. 3 shows, the quantities of the basic surface sites always appear higher than the amount of the acidic surface sites. The number of basic surface sites increases to a maximum at around 50% burn-off and then decreases. The number of acidic sites remains practically constant until the burn-off up to 40.5%, then it decreases obviously. Furthermore, the activated carbons prepared at lower temperature (850 °C) have larger quantities of the basic surface sites than that produced at higher temperatures (900 and 950 °C), while the number of the acidic sites seems to be equivalent.

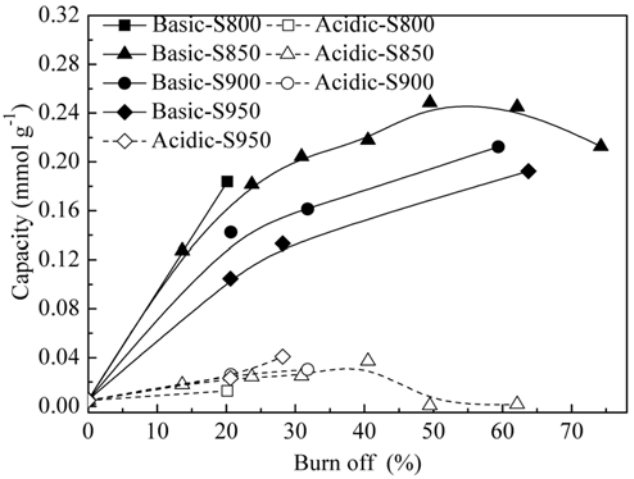

Fig. 3. Quantity of surface sites with acidic and basic characteristics of activated carbons.

When H_2O molecule comes in contact with the char, the chemisorbed oxygen and oxygen transfer between reacting gas and carbon atoms occurs in the C-H_2O reaction. Activation with H_2O leaves in the carbon structure a large number of oxygen surface groups with acidity or basicity. The question on the structure of chemisorbed oxygen and fleeting oxygen groups in the C-H_2O reaction remained unresolved in our experiments. It is possible that many acidic surface sites were built in the C-H_2O reaction, but most of them were unstable at high activation temperatures and decomposed to form basic sites. So the basic surface sites could be the formation of oxygen transfer in the C-H_2O reaction or decomposition of acidic sites.

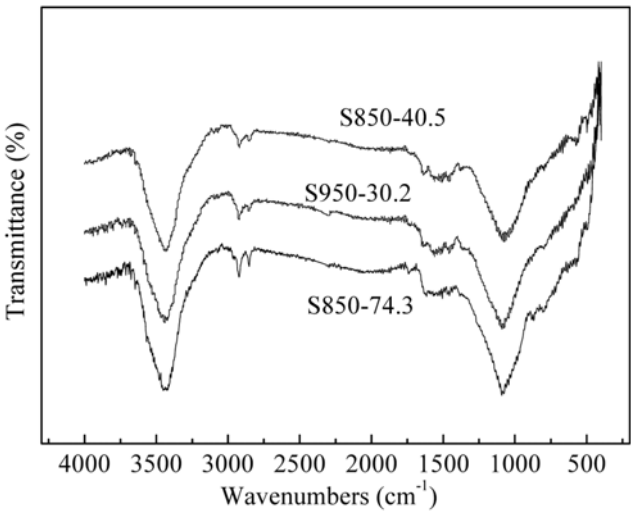

Fig. 4. FTIR spectra of activated carbons.

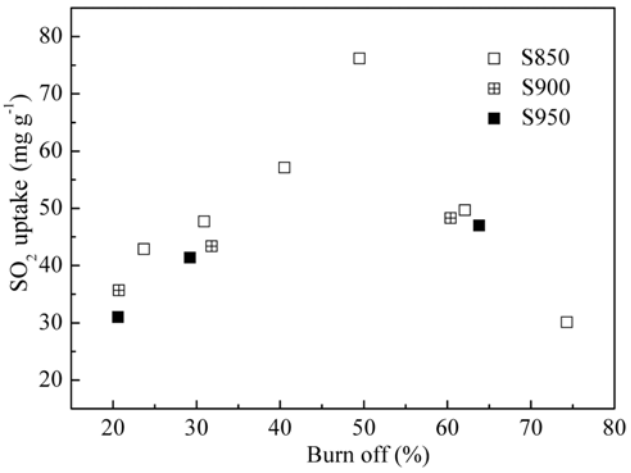

Fig. 5. SO_2 adsorption capacity on activated carbons versus burn-off and temperature.

The surface chemistry of the activated carbon is evaluated by FTIR (Fig. 4). It presents the spectra of samples obtained via different activation temperatures and burn-offs. All spectra have similar absorption bands, being only the difference in their intensities and a slight shift in wavenumbers, which indicates just small differences in the surface chemistry. The assignment of a specific wavenumber to a given functional group could not be possible, because the absorption bands of various functional groups are overlapped. In the spectrum, the broad band in the 3,600-3,250 cm^{-1} can be attributed to O-H stretching vibrations in hydroxyl, carboxylic, and phenolic groups. The presence of band between 3,000 and 2,700 cm^{-1} represents aliphatic CH, CH_2, CH_3 stretching modes. The 1,750-1,420 cm^{-1} is associated with C=O stretching vibrations in carboxylic acids, lactones, esters, and quinones. The 1,300-1,000 cm^{-1} band is assigned to the C-O stretching vibrations, C-O-C, O-H bending modes in carboxylic acids, carboxyl, lactones, esters, and ethers. The pyrone groups formed by rearrangement of adjacent ether and carboxyl present relatively strong basicity and they have strong affinity for acidic molecules such as SO_2 [23].

3. Study of SO_2 Adsorption

The amount of SO_2 adsorbed at 80 °C from a simulated flue gas for AC sample is shown in Fig. 5. For 850 °C activation, there is

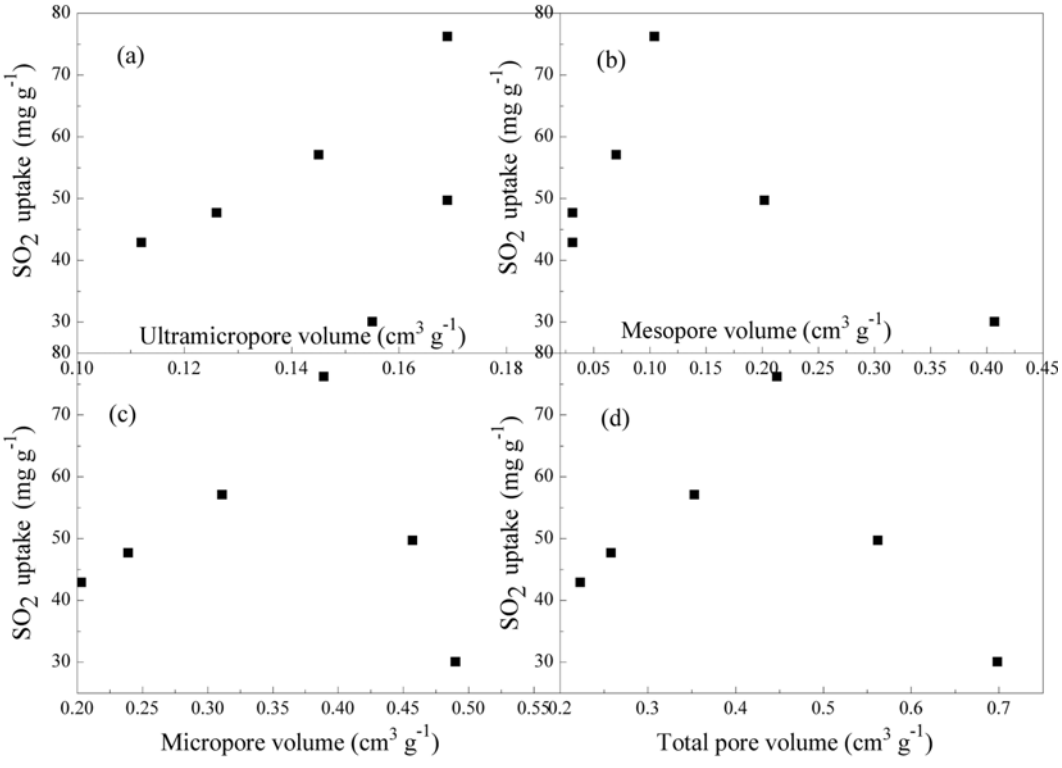

Fig. 6. Relationship between the SO_2 capacity and the pore volumes.

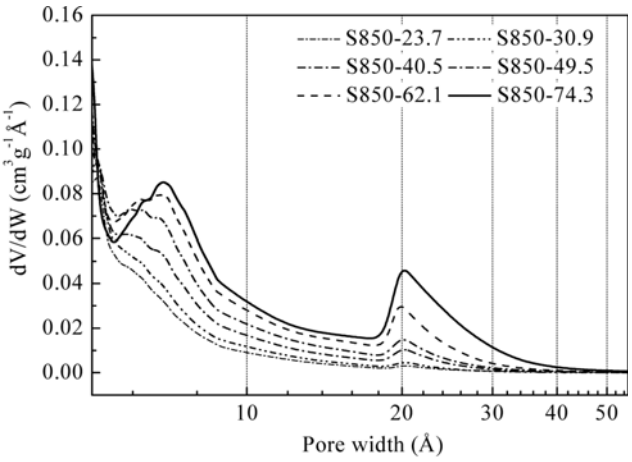

Fig. 7. Pore size distribution of activated carbons.

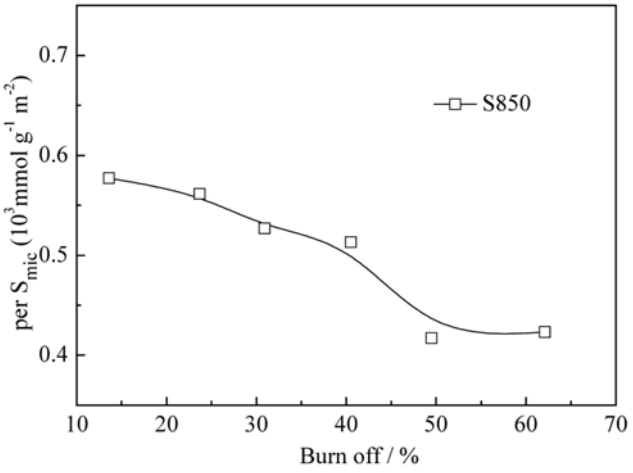

Fig. 8. Relationship between the number of surface sites per S_{mic} and the burn-off.

an obvious relationship between the SO_2 adsorption and burn-off degree. The SO_2 capacity increases linearly until 50% burn-off, and then it decreases drastically with increasing burn-off. Additionally, the AC samples produced at lower temperature present a little higher SO_2 capacities than those prepared at higher temperature. These results are considered to be associated with pore volume, pore size distribution and quantities of the basic surface sites of the AC sample.

The plot of the amount of SO_2 adsorbed versus different pore volumes is given in Fig. 6. As it can be seen, there seems to be a linear relationship between the amount of SO_2 adsorbed and the micropore and total pore volumes within a certain range. In other words, when the V_{mic} and V_{tot} are low, the SO_2 capacity increases with increasing pore volumes. However, the amount of SO_2 adsorbed tends to decrease as the V_{mic} and V_{tot} continuously increase. The influence of ultramicropore volume on SO_2 capacity presents a similar trend with that of V_{mic} and V_{tot}, that is, a higher pore volume is not necessary to obtain better SO_2 adsorption capacity. In contrast, there is not a clear relationship between the mesopore volume and the amount of SO_2 adsorbed as Fig. 6(b) shows. According to these conclusions, evaluation of SO_2 adsorption capacity just based on pore volumes is not enough. The pore size distribution and surface chemistry will also play an important role in the adsorption of SO_2 on activated carbon.

Compared with specific surface area and pore volume, pore size distribution can describe the nature of a porous structure in more detail [24]. Fig. 7 exhibits pore size distributions of some resulting activated carbons. Generally speaking, there is a very similar trend in all the figures that pores are mainly during the range around 5-9 Å. In more detail, we can see that in the pore size distribution of each activated carbon appears a small peak around 20 Å. With an increase of burn-off, the small peak increases rapidly and the range expands from 20 to 30 Å, especially for around 70% burn-off.

As described by Fig. 6, the micropore structure has more significant influence on SO_2 capacities of AC samples than the mesopore structure. It is important to notice that the position of the main peak shifts to larger pore dimensions with an increase in burn-off, specifically, pores around 6 Å of S850-62.1 and S850-74.3 are obviously lower than that of S850-49.5. This result for pore structure presented by pore size distributions is in agreement with that described by median pore diameters which increase with increasing burn-off. For series AC samples, the smaller pores have a high affinity for adsorption of SO_2, so pore widening with high burn-off reduces physical energy, thus making low adsorption of SO_2. Although the micropore and mesopore volumes increase with increasing burn-off, the SO_2 adsorption capacities of activated carbons decrease. It could be assumed that a large micropore volume does not necessarily assure an optimal adsorption of SO_2 and gases; rather, the pore size and pore size distribution should be considered as important parameters. In our case, the steam activation with high burn-off leads to a larger dimension pore size distribution and median pore diameter, so that the SO_2 capacities of AC samples are reduced.

As Fig. 5 shows, the activated carbons prepared at different temperatures represent different SO_2 adsorption capacities. It is proved that the result is in agreement with analysis of AC samples with different burn-offs.

Generally, the adsorption capacity for SO_2 is dependent on both the pore structure and the surface chemistry. In a series of activated carbons, the surface groups are similar and the number is associated with micropore area and volume. The quantities of surface sites per micropore area (S_{mic}) are calculated and shown in Fig. 8. It shows that the quantities of surface sites per S_{mic} decrease with an increase in burn-off, and the difference is neglectable compared with development of pore structures. As a result, we considered that the results of SO_2 adsorption are mainly attributed to pore structures in this work.

CONCLUSIONS

The effects of activation conditions on the textural and chemical properties of the AC samples were studied, and the physico-chemical properties of the activated carbons on the SO_2 adsorption were also investigated. For steam activation the increasing burn-off leads to AC samples with continuous evolution of all types of pores except ultramicropore. For 850 °C activation the ultramicropore increases to a maximum of 0.169 cm^3/g at around 50% burn-off and then decrease. It can be concluded that steam produces an increase in ultramicropore in the early stages of activation, whereas it is more

effective in micropore widening with high burn-off degree. Furthermore, it is deduced that widening of existing ultramicropores occurs during the whole stage of activation based on continuous development in supermicropore. It is shown that the micropore of activated carbons decreased and the mesopore increased by increasing activation temperature. This means that the faster reaction is prone to external burn-off and only the most accessible pore structure at higher temperature. For all the resulting AC samples, the amount of the basic surface sites always appears much higher than the amount of the acidic sites.

It is observed that there was some relationship between SO_2 adsorption and the textural properties of AC samples. There seems to be a linear relationship between the amount of SO_2 adsorbed and the micropore volumes within a certain range. It can be concluded that a higher pore volume is not necessary to obtain better SO_2 adsorption capacity. The pore size and pore size distribution should be considered as important parameters on SO_2 adsorption. In our case, the steam activation with high burn-off leads to a larger dimension pore size distribution and median pore diameter that reduces SO_2 capacities of AC samples.

ACKNOWLEDGEMENTS

The authors gratefully acknowledge the National High Technology Research and Development program of China (Grant No. 2007AA05Z307).

REFERENCES

1. J. Y. Rau, H. H. Tseng, B. C. Chiang, M. Y. Wey and M. D. Lin, *Fuel*, **89**, 732 (2010).
2. Z. Q. Li, S. B. Fan, G. K. Liu, X. H. Yang, Z. C. Chen, W. Su and L. Wang, *Energy Fuels*, **24**, 38 (2010).
3. T. J. Li, Y. Q. Zhuo, J. Y. Lei and X. C. Xu, *Korean J. Chem. Eng.*, **24**, 1113 (2007).
4. Y. Wang, Z. Huang, Z. Liu and Q. Liu, *Carbon*, **42**, 445 (2004).
5. D. López, R. Buitrago, A. Sepñlveda-Escribano, F. Rodríguez-Reinoso and F. J. Mondragón, *Phys. Chem. C*, **112**, 15335 (2008).
6. E. Raymundo-Piòero, D. Cazorla-Amorós and A. Linares-Solano, *Carbon*, **39**, 231 (2001).
7. P. Davini, *Carbon*, **39**, 1387 (2000).
8. A. A. Lizzio and J. A. DeBarr, *Fuel*, **75**, 1515 (1996).
9. H. Y. Kang, S. S. Park and Y. S. Rim, *Korean J. Chem. Eng.*, **23**, 948 (2006).
10. G Chattopadhyaya, D. G Macdonald, N. N. Bakhshi and A. K. Dalai, *Fuel Process. Technol.*, **87**, 997 (2006).
11. Y. Ngernyen, C. Tangsathitkulchai and M. Tangsathitkulchai, *Korean J. Chem. Eng.*, **23**, 1046 (2006).
12. S. B. Lyubchik, R. Benoit and F. Béguin, *Carbon*, **40**, 1287 (2001).
13. M. Belhachemi, R. V. R. A. Rios, F. Addoun, J. Silvestre-Albero, A. Sepúlveda-Escribano and F. J. Rodríguez-Reinoso, *Anal. Appl. Pyrolysis*, **86**, 168 (2009).
14. R. Pietrzak, *Fuel*, **88**, 1871 (2009).
15. M. T. Izquierdo, B. Rubio, C. Mayoral and J. M. Andrés, *Fuel*, **82**, 147 (2003).
16. A. A. Lizzio and J. A. DeBarr, *Energy Fuels*, **11**, 284 (1997).
17. M. A. Daley, C. L. Magnum, J. A. DeBarr, S. Riha, A. A. Lizzio, G. L. Donnals and J. Economy, *Carbon*, **35**, 411 (1997).
18. F. Rodríguez-Reinoso, M. Molina-Sabio and M. T. González, *Carbon*, **33**, 15 (1995).
19. J. Pastor-Villegas and C. J. Durán-Valle, *Carbon*, **40**, 397 (2002).
20. D. López, R. Buitrago, A. Sepñlveda-Escribano, F. Rodríguez-Reinoso and F. J. Mondragón, *Phys. Chem. C*, **111**, 1417 (2007).
21. C. L. Mangun, J. A. DeBarr and J. Economy, *Carbon*, **39**, 1689 (2001).
22. S. A. C. Carabineiro, A. M. Ramos, J. Vital, J. M. Loureiro, J. J. M. Órfão and I. M. Fonseca, *Catal. Today*, **78**, 203 (2003).
23. H. P. Boehm, *Carbon*, **32**, 759 (1994).
24. M. Seredych, E. Deliyanni and T. J. Bandosz, *Fuel*, **89**, 1499 (2010).